The Mesoproterozoic Maz terrane in the Western Sierras Pampeanas, Argentina, equivalent to the Arequipa–Antofalla block of southern Peru? Implications for West Gondwana margin evolution

C. Casquet [a,*], R.J. Pankhurst [b], C.W. Rapela [c], C. Galindo [a], C.M. Fanning [d], M. Chiaradia [e], E. Baldo [f], J.M. González-Casado [g], J.A. Dahlquist [f]

[a] *Departamento de Petrología y Geoquímica, Universidad Complutense, 28040 Madrid, Spain*
[b] *British Geological Survey, Keyworth, Nottingham NG12 5GG, United Kingdom*
[c] *Centro de Investigaciones Geológicas, Universidad Nacional de La Plata, 1900 La Plata, Argentina*
[d] *Research School of Earth Sciences, The Australian National University, Canberra, Australia*
[e] *Section des Sciences de la Terre, Département de Minéralogie, Université de Genève, CH-1205 Genève, Switzerland*
[f] *Departamento de Geología, Universidad Nacional de Córdoba, 5000 Córdoba, Argentina*
[g] *Departamento Química Agrícola, Geología y Geoquímica, Universidad Autónoma, 28049 Madrid, Spain*

Abstract

The rocks of Sierra de Maz and Sierra del Espinal (Western Sierras Pampeanas) represent pre Famatinian (Ordovician) basement. Isotope compositions (Nd and Pb) of metasedimentary rocks and SHRIMP U Pb dating of detrital zircons, combined with other geological evidence, show that three parallel N S domains can be recognized. The central Maz Domain contains pre Grenvillian metasedimentary rocks deposited between 1.2 and 1.6 Ga, that underwent Grenvillian granulite facies metamorphism and were intruded by mafic igneous rocks and massif-type anorthosites. Metasedimentary rocks have high Nd T_{DM} ages (1.7 2.7 Ga) and very radiogenic Pb (μ 9.8 10.2), suggesting provenance from reworked early Proterozoic or Archean continental crust. The domains to the east and west of the Maz Domain consist of three metasedimentary sequences with Nd T_{DM} ages between 1.2 and 1.6 Ga and variably radiogenic Pb (μ=9.6 10.0). U Pb SHRIMP dating of detrital zircons, Nd T_{DM} model ages and comparison with other data suggest that these sequences are post Grenvillian, i.e., Neoproterozoic and/or early Paleozoic.

The Maz Domain is interpreted as a suspect terrane similar to the northern Arequipa Antofalla craton that forms the basement of the Central Andes; both underwent Grenville age orogeny and were probably once continuous along the western margin of Amazonia (West Gondwana).

Keywords: Sierras Pampeanas; U–Pb SHRIMP zircon dating; Nd isotopes; Pb isotopes; Gondwana; Grenville

1. Introduction

The Western Sierras Pampeanas and the Arequipa Antofalla basement of the central Andes (Fig. 1) constitute two large exposures of pre-Andean rocks where tectonothermal activity of Grenville age (1.0–1.2 Ga) has been recognized. However, correlation between these two domains remains hampered because of insufficient geological, isotope and geochronological knowledge. The Grenville orogeny allegedly led to amalgamation of existing continental masses into the Rodinia supercontinent (Piper, 1976). Recent paleogeographical reconstructions of Rodinia at c. 1.0 Ga place Laurentia facing the Amazonia and Kalahari cratons, with a small Arequipa Antofalla block between these two cratons and a continuous Grenville belt that joins all four continental masses and extends into the Musgrave and Albany Fraser mobile belts in Australia (Wingate et al., 1998; Loewy et al., 2003). To date these models do not take account of the Western Sierras Pampeanas.

* Corresponding author.
E-mail address: casquet@geo.ucm.es (C. Casquet).

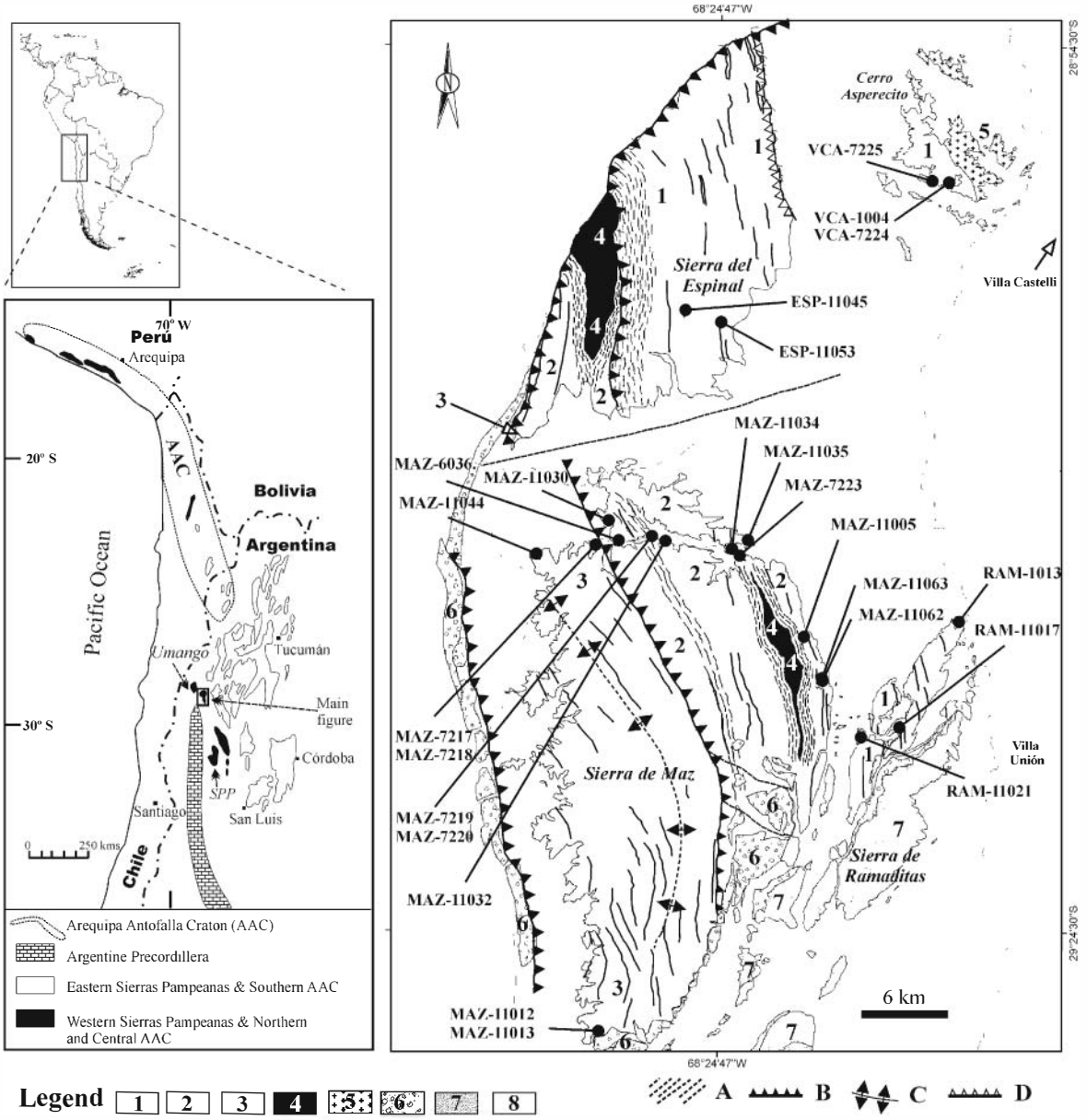

Fig. 1. Location of the Sierras Pampeanas and of the Arequipa–Antofalla craton (AAC) with location of samples considered in this work. WSP, Western Sierras Pampeanas; ESP, Eastern Sierras Pampeanas; PC, Argentine Precordillera; SPP, Sierra de Pie de Palo. Main figure shows a geological sketch map of the Sierra de Maz and surrounding areas referred to in the text. Crystalline basement: (1) Eastern Domain; (2) Maz Domain; (3) Western Domain; (4) massif-type anorthosites; (5) Famatinian plutons; (6) Upper Paleozoic sedimentary cover; (7) Mesozoic cover; (8) Cenozoic cover. (A) Ductile shear zones; (B) pre-Andean thrusts; (C) anticline; (D) Andean thrusts. Full lines: foliation trends.

We provide here new Nd and Pb isotope compositions and U–Pb SHRIMP zircon data from the Western Sierras Pampeanas (Sierra de Maz, Sierra del Espinal and adjoining sierras). These data suggest the outline of a new terrane of Mesoproterozoic age that underwent Grenville-age orogeny. Moreover, this terrane shows isotopic and geological similarities with the central and northern part of the Arequipa–Antofalla craton of Peru and northern Chile, and Amazonia, suggesting that they were probably all once part of a continuous belt of Grenvillian reworked basement largely autochthonous to Amazonia (Western Gondwana). The Maz suspect terrane is tectonically imbricated with post-Grenvillian terranes, probably as a consequence of the Famatinian (i.e. Ordovician) orogeny and younger faulting.

2. Geologic outline of the Central Andes basement

The Sierras Pampeanas of central western Argentina constitute the largest outcrop of pre-Mesozoic crystalline basement in central Andean South America. There is consensus that most of the pre-Andean evolution of this region resulted from protracted plate interaction along the proto-Andean margin of Gondwana over a long period of time, from as early as Mesoproterozoic to Late Paleozoic (e.g., Rapela et al., 1998a; Ramos, 2004, and references therein; Baldo et al., 2006). This tectonothermal activity continued throughout today. At least two discrete orogenic belts of Paleozoic age have been recognized, i.e. the Early Cambrian Pampean belt in the eastern sierras and the Ordovician

Famatinian belt in the central and western sierras, partially overprinting the former (e.g., Rapela et al., 1998b). In the central and eastern Sierras Pampeanas both orogenies involved predominantly Late Ne proterozoic sedimentary rocks and were accompanied by low- to high-grade metamorphism, magmatism and foliation development.

U–Pb zircon evidence of Famatinian-rejuvenated Proterozoic terranes of Grenvillian age (1.0 to 1.2 Ga) in the Western Sierras Pampeanas was first found in the Sierra de Pie de Palo (McDonough et al., 1993; Casquet et al., 2001; Vujovich et al., 2004). This region became the subject of much interest in recent years after the hypothesis was laid that the Famatinian orogeny was the result of collision of Laurentia with the proto-Andean margin of Gondwana (Dalla Salda et al., 1992). This hypothesis was sustained by the fact that the Argentine Precordillera, west of the Sierras Pampeanas, contains a sedimentary sequence of Early to Middle Paleozoic age, starting with a Cambrian to earliest Mid-Ordovician carbonate platform with benthic faunas of Laurentian affinity (e.g., Benedetto, 1998, and references therein). Further work led to the paleogeographically more restrictive model that the Famatinian colliding terrane was in fact a smaller exotic block — the Precordillera terrane, allegedly derived from the Ouachita embayment in Laurentia (Astini et al., 1995; Thomas and Astini, 1996). The Sierra de Pie de Palo has been taken as the easternmost exposure of the basement of the Precordillera cover sequence (e.g., Ramos, 2004) — xenoliths of Grenville age are also found in Miocene volcanic rocks of the Precordillera (Kay et al., 1996). However the present extent of the Precordillera terrane remains a matter of debate (e.g. Galindo et al., 2004; Ramos, 2004; Rapela et al., 2005).

The recent finding of massif-type anorthosites of Grenvillian age (c. 1.08 Ga) in the Sierra de Maz and Sierra del Espinal (Casquet et al., 2005a), and of granitic orthogneisses of similar age (ca. 1.1 Ga) in the nearby Sierra de Umango (Varela et al., 2003), implies that Mesoproterozoic rocks extended further north than previously supposed. Moreover, age and chemical similarities between the Maz and Espinal anorthosites and those of the Appalachian margin of Laurentia led Casquet et al. (2005a) to suggest that the Western Sierras Pampeanas Grenvillian basement was once part of a now-disrupted continuous Grenvillian belt. Proof of a Grenvillian orogeny in the Western Sierras Pampeanas, represented by granulite facies metamorphism of c. 1.2 Ga, has been recognized in Mesoproterozoic metasedimentary rocks of Sierra de Maz (Casquet et al., 2006). Preliminary isotope data further led to correlation between the Maz–Espinal Grenville-age basement and the central and northern Arequipa–Antofalla craton (Casquet et al., 2005a,b).

The Arequipa–Antofalla craton (Ramos, 1988) is known from scattered inliers of rocks of Proterozoic and Early Paleozoic age exposed through the Andean Mesozoic to Cenozoic sedimentary and volcanic cover. Outcrops occur in Peru, Bolivia, northern Chile and northern Argentina (Fig. 1). The Arequipa–Antofalla craton is interpreted to be exotic and was apparently accreted to the main craton Amazonia to the east during the Sunsas orogeny at c. 1.0 Ga (e.g., Loewy et al., 2004). The northern (Arequipa Massif) and central part of the Arequipa–Antofalla craton consists of Mesoproterozoic metasedimentary and metavolcanic rocks and orthogneisses, the latter with peak U–Pb zircon crystallization ages of approximately 1.9–1.8 Ga (northern domain) and 1.2–1.05 Ga (central domain) (Damm et al., 1990; Wasteneys et al., 1995; Loewy et al., 2004). Grenville-age medium- to high-grade (granulite) metamorphism and deformation between c. 1.2 Ga and c. 950 Ma overprinted both domains (Wasteneys et al., 1995; Martignole and Martelat, 2003; Loewy et al., 2004). The region further underwent Famatinian metamorphism and magmatism in the Ordovician, between 470 and 440 Ma (Loewy et al., 2004). Remarkably Grenvillian massif-type anorthosites, part of an AMGC suite, have been recently disc vered at Ilo (Peru) in the northern domain (Martignole et al., 2005) that are very similar to those of Western Sierras Pampeanas. The southern part of the Arequipa–Antofalla craton differs significantly from the other two domains. It consists of several inliers, for the most part no more than weakly metamorphosed, Early Paleozoic sedimentary and volcanic rocks. Granitic plutons of Famatinian age and younger are common with U–Pb zirc n crystallization ages between c. 450 Ma and c. 270 Ma (Damm et al., 1990).

3. Geologic setting of the Sierra de Maz and Sierra del Espinal

We include here the two main sierras but also the nearby Sierra de Ramaditas and the Villa Castelli isolated massif (Fig. 1). The sierras of Maz and Ramaditas were first described by Kilmurray and Dalla Salda (1971). Taken together they constitute a NNW–SSE trending belt of metamorphic rocks ranging from high-grade in the east to low-grade in the west. An eastward-dipping tectonic foliation is always present, dip values decreasing regularly westward in a fan-like arrangement from near vertical to subhorizontal. Three parallel domains can be recognized on field and geochemical evidence (see below), separated by first order shear zones and faults that produce metamorphic discontinuities (Fig. 1). The Eastern Domain embraces the eastern Sierra del Espinal, the Sierra de las Ramaditas and the Villa Castelli massifs. It consists of widespread garnet–sillimanite migmatitic paragneisses and local marbles and amphibolites of unknown age, assigned by Kilmurray and Dalla Salda (1971) to their El Tac Group of metasedimentary rocks. The Central Domain (henceforth referred to as the Maz Domain) crops out in central and eastern Sierra de Maz and western Sierra del Espinal. It consists of a complex sequence of medium-grade (kyanite–sillimanite–garnet–staurolite schists, quartzites, amphibolites and very scarce marbles) to high-grade mafic and meta-pelitic rocks with interleaved quartzites and minor marble lenses. Relics of mafic granulites and serpentinites have been recognized among the latter, granulite facies metamorphism having been dated as of Grenville age (c. 1.2 Ga; Casquet et al., 2006). Detrital zircon U–Pb SHRIMP ages constrain the sedimentation age of one garnet schist that underwent granulite facies metamorphism to the Mesoproterozoic (between c. 1.7 and 1.2 Ga), with Paleoproterozoic provenance ages (Casquet et al., 2006). More ver, the massif-type anorthosites referred to above are only found in the Maz Domain (Fig. 1). Other rock types of the Maz Domain include orthogneisses, Grenville-age meta-diorites (Casquet et al.,

Table 1
Summary of SHRIMP U–Pb zircon results for samples MAZ-11063 and RAM-1013

Grain. spot	U (ppm)	Th (ppm)	Th/U	Pb* (ppm)	$^{204}Pb/^{206}Pb$	f_{206}%	Total ratios				Radiogenic ratios						ρ	Age (Ma)				
							$^{238}U/^{206}Pb$	±	$^{207}Pb/^{206}Pb$	±	$^{206}Pb/^{238}U$	±	$^{207}Pb/^{235}U$	±	$^{207}Pb/^{206}Pb$	±		$^{206}Pb/^{238}U$	±	$^{207}Pb/^{206}Pb$	±	%Disc
1) RAM-1013																						
SHRIMP II																						
1.1r	133	25	0.19	8	0.000301	0.16	13.752	0.177	0.0572	0.0011	0.0726	0.0010						452	6			
1.2c	73	20	0.28	16	0.000361	0.59	3.927	0.052	0.0957	0.0011	0.2532	0.0034	3.165	0.068	0.0907	0.0015	0.625	1455	17	1440	32	−1
2.1c	139	156	1.13	28	–	<0.01	4.251	0.052	0.0892	0.0008	0.2353	0.0029	2.904	0.045	0.0895	0.0008	0.801	1362	15	1415	18	4
2.2r	97	8	0.08	6	–	0.28	14.251	0.193	0.0578	0.0014	0.0700	0.0010						436	6			
3.1c	149	62	0.42	29	0.000151	0.25	4.431	0.054	0.0883	0.0008	0.2251	0.0027	2.677	0.054	0.0862	0.0014	0.601	1309	14	1343	31	3
3.2r	107	24	0.23	6	0.000540	0.49	14.402	0.208	0.0594	0.0015	0.0691	0.0010						431	6			
4.1c	163	83	0.51	24	0.000148	0.25	5.767	0.070	0.0752	0.0008	0.1730	0.0021	1.742	0.031	0.0730	0.0010	0.669	1028	11	1015	27	−1
4.2r	94	15	0.16	6	0.000109	0.71	14.251	0.197	0.0613	0.0015	0.0697	0.0010						434	6			
5.1c	155	80	0.51	22	0.000087	0.15	5.981	0.073	0.0750	0.0008	0.1669	0.0020	1.699	0.035	0.0738	0.0012	0.590	995	11	1036	34	4
5.2c	424	385	0.91	66	–	<0.01	5.527	0.062	0.0754	0.0005	0.1810	0.0020	1.895	0.025	0.0759	0.0006	0.832	1073	11	1093	15	2
6.1r	284	67	0.24	18	0.000111	0.19	13.812	0.162	0.0575	0.0008	0.0723	0.0009						450	5			
7.1r	144	18	0.12	9	–	0.25	14.135	0.184	0.0577	0.0011	0.0706	0.0009						440	6			
8.1c	172	71	0.41	26	0.000074	0.12	5.650	0.068	0.0771	0.0008	0.1768	0.0021	1.855	0.047	0.0761	0.0017	0.481	1049	12	1098	44	5
9.1c	211	127	0.60	31	–	<0.01	5.883	0.069	0.0760	0.0007	0.1700	0.0020	1.786	0.027	0.0762	0.0007	0.778	1012	11	1100	19	9
9.2r	134	31	0.23	8	0.000486	0.44	14.045	0.182	0.0593	0.0015	0.0709	0.0009						441	6			
10.1r	151	50	0.33	9	0.000635	0.24	13.972	0.180	0.0577	0.0011	0.0714	0.0009						445	6			
11.1c	278	103	0.37	44	–	<0.01	5.391	0.068	0.0769	0.0006	0.1855	0.0023	1.967	0.029	0.0769	0.0006	0.856	1097	13	1119	15	2
11.2r	109	25	0.23	6	0.000551	0.52	14.544	0.203	0.0596	0.0014	0.0684	0.0010						426	6			
12.1r	283	48	0.17	18	–	0.16	13.479	0.159	0.0575	0.0008	0.0741	0.0009						461	5			
13.1r	147	22	0.15	15	0.010054	19.28	8.709	0.130	0.2165	0.0061	0.0936	0.0030						577	18			
14.1r	124	140	1.13	10	0.000358	0.43	11.136	0.151	0.0621	0.0013	0.0894	0.0012						552	7			
15.1r	246	15	0.06	17	0.000154	0.05	12.113	0.149	0.0579	0.0009	0.0825	0.0010						511	6			
16.1c	147	61	0.41	23	0.000159	0.27	5.483	0.069	0.0767	0.0009	0.1819	0.0023	1.868	0.042	0.0745	0.0014	0.565	1077	13	1054	37	−2
17.1c	323	157	0.49	62	0.000058	0.10	4.483	0.063	0.0848	0.0006	0.2228	0.0032	2.581	0.047	0.0840	0.0009	0.783	1297	17	1293	22	0
18.1c	167	43	0.26	43	–	<0.01	3.296	0.043	0.1126	0.0008	0.3035	0.0040	4.720	0.070	0.1128	0.0008	0.877	1709	20	1845	13	8
19.1r	117	22	0.19	7	0.000426	0.40	14.098	0.199	0.0589	0.0015	0.0706	0.0010						440	6			
19.2c	297	141	0.47	42	0.000030	0.05	6.087	0.073	0.0743	0.0007	0.1642	0.0020	1.673	0.032	0.0739	0.0011	0.631	980	11	1039	30	6
20.1c	359	104	0.29	54	0.000089	0.15	5.681	0.065	0.0771	0.0006	0.1758	0.0020	1.838	0.028	0.0758	0.0008	0.752	1044	11	1090	20	4
21.1r	108	1	0.01	7	0.000427	0.45	14.063	0.200	0.0593	0.0015	0.0708	0.0010						441	6			
21.2c	170	102	0.60	26	0.000268	0.45	5.692	0.070	0.0778	0.0009	0.1749	0.0022	1.784	0.063	0.0740	0.0024	0.360	1039	12	1041	66	0
22.1r	247	45	0.18	16	0.000192	0.27	13.598	0.213	0.0583	0.0010	0.0733	0.0012						456	7			
23.1r	116	30	0.26	7	0.000999	0.42	14.230	0.198	0.0590	0.0014	0.0700	0.0010						436	6			
24.1r	135	51	0.37	8	0.000613	0.17	13.780	0.291	0.0574	0.0013	0.0724	0.0016						451	9			
25.1r	159	34	0.22	10	0.000368	0.23	13.407	0.178	0.0582	0.0012	0.0744	0.0010						463	6			
25.2c	103	40	0.39	18	0.000030	0.05	4.957	0.066	0.0820	0.0011	0.2016	0.0027	2.267	0.064	0.0815	0.0020	0.478	1184	15	1234	49	4
26.1c	61	35	0.57	9	0.000362	0.62	5.580	0.086	0.0779	0.0015	0.1781	0.0028	1.785	0.060	0.0727	0.0022	0.456	1057	15	1006	61	−5
SHRIMP RG, mount repolished																						
2.3r	319	45	0.14	44	0.000054	1.08	6.166	0.073	0.0801	0.0005	0.1620	0.0019	1.772	0.024	0.0793	0.0006	0.861	968	11	1180	14	22
1.3r	134	20	0.15	8	0.000041	0.11	14.274	0.176	0.0565	0.0010	0.0700	0.0009						436	5			
19.3r	107	22	0.20	6	0.000047	0.07	14.479	0.185	0.0560	0.0011	0.0690	0.0009						430	5			
7.2r	133	21	0.16	8	0.000037	0.12	13.613	0.210	0.0571	0.0010	0.0734	0.0012						456	7			
28.1r	176	27	0.15	13	0.000195	1.13	11.543	0.134	0.0672	0.0008	0.0857	0.0010						530	6			
29.1r	112	20	0.18	7	0.000035	0.73	13.715	0.217	0.0619	0.0011	0.0724	0.0012						450	7			
9.3r	137	29	0.21	8	–	0.10	13.822	0.168	0.0567	0.0010	0.0723	0.0009						450	5			

10.2r	122	29	0.24	8	0.000005	0.07	13.820	0.171	0.0565	0.0010	0.0723	0.0009						450	5		
21.3r	116	10	0.09	7	–	0.09	14.428	0.209	0.0562	0.0010	0.0692	0.0010						432	6		
11.3r	94	23	0.25	6	–	0.32	13.865	0.184	0.0584	0.0012	0.0719	0.0010						448	6		
30.1r	103	26	0.25	6	0.000128	0.25	13.928	0.182	0.0579	0.0012	0.0716	0.0010						446	6		
22.2r	197	52	0.27	12	0.000279	0.17	14.096	0.165	0.0571	0.0008	0.0708	0.0008						441	5		
31.1r	117	27	0.23	7	0.000124	0.34	14.435	0.202	0.0582	0.0011	0.0690	0.0010						430	6		
23.2r	105	27	0.26	6	0.000073	0.43	14.209	0.182	0.0591	0.0011	0.0701	0.0009						437	6		
24.2r	141	60	0.43	9	–	0.27	13.779	0.169	0.0581	0.0010	0.0724	0.0009						450	5		
25.3r	133	23	0.17	8	0.000224	0.06	14.378	0.178	0.0560	0.0010	0.0695	0.0009						433	5		
32.1r	72	20	0.28	5	0.000077	0.43	12.345	0.171	0.0608	0.0013	0.0807	0.0011						500	7		
34.1r	124	30	0.24	8	0.000023	0.26	13.982	0.173	0.0579	0.0010	0.0713	0.0009						444	5		
33.1r	201	27	0.13	13	0.000270	0.06	13.460	0.216	0.0567	0.0008	0.0742	0.0012						462	7		

Notes

1. r = rim, c = core.
2. Uncertainties given at the 1σ level.
3. f_{206} % denotes the percentage of ^{206}Pb that is common Pb.
4. Error in AS3 reference zircon calibration was 0.59% and 0.58% for the two analytical sessions (not included in above errors but required when comparing data from different mounts).
5. Correction for common Pb made using the measured ^{204}Pb/^{206}Pb ratio.
6. For % Conc., 0% denotes a concordant analysis.

a) MAZ11043

1.1	206	81	0.39	32	0.000061	0.10	5.485	0.067	0.0776	0.0009	0.1821	0.0022	1.928	0.034	0.0768	0.0010	0.693	1079	12	1115	25 3
2.1	53	51	0.96	9	0.000299	0.51	5.242	0.089	0.0785	0.0015	0.1898	0.0032	1.942	0.061	0.0742	0.0020	0.541	1120	17	1047	53 −7
3.1	103	34	0.33	16	0.000298	0.51	5.525	0.078	0.0778	0.0011	0.1802	0.0025	1.842	0.040	0.0741	0.0012	0.657	1068	15	1046	33 −2
4.1	25	26	1.04	4	–	<0.01	5.208	0.112	0.0747	0.0019	0.1923	0.0041	2.008	0.069	0.0757	0.0020	0.626	1134	22	1088	54 −4
5.1	501	680	1.36	72	0.000189	0.32	5.994	0.090	0.0777	0.0005	0.1663	0.0025	1.719	0.032	0.0750	0.0008	0.819	992	14	1068	21 7
6.1	341	87	0.26	152	0.000020	0.03	1.929	0.022	0.2187	0.0034	0.5182	0.0060	15.610	0.302	0.2185	0.0034	0.601	2691	26	2970	25 9
7.1	502	258	0.51	77	–	<0.01	5.610	0.065	0.0783	0.0006	0.1782	0.0021	1.923	0.027	0.0783	0.0006	0.822	1057	11	1154	16 8
8.1	458	66	0.14	81	–	<0.01	4.835	0.055	0.0810	0.0006	0.2069	0.0024	2.316	0.031	0.0812	0.0006	0.850	1212	13	1226	14 1
9.1	243	84	0.35	37	0.000035	0.06	5.622	0.070	0.0747	0.0008	0.1778	0.0022	1.819	0.030	0.0742	0.0008	0.760	1055	12	1048	21 −1
10.1	106	89	0.84	30	–	<0.01	3.002	0.049	0.1165	0.0011	0.3331	0.0054	5.353	0.101	0.1165	0.0011	0.858	1854	26	1904	17 3
11.1	157	91	0.58	26	0.000111	0.19	5.135	0.069	0.0757	0.0009	0.1944	0.0026	1.987	0.045	0.0741	0.0013	0.596	1145	14	1045	37−10
12.1	164	85	0.52	27	–	<0.01	5.221	0.069	0.0777	0.0009	0.1918	0.0025	2.084	0.040	0.0788	0.0011	0.688	1131	14	1167	28 3
13.1	141	69	0.49	22	0.000062	0.10	5.494	0.083	0.0770	0.0010	0.1818	0.0027	1.908	0.038	0.0761	0.0010	0.753	1077	15	1099	26 2
14.1	201	242	1.21	30	0.000584	0.99	5.823	0.082	0.0825	0.0012	0.1700	0.0024	1.740	0.065	0.0742	0.0026	0.381	1012	13	1047	70 3
15.1	66	25	0.38	21	0.000532	0.79	2.672	0.045	0.1424	0.0017	0.3714	0.0064	6.935	0.186	0.1354	0.0028	0.641	2036	30	2170	36 6
16.1	58	27	0.47	9	0.000403	0.70	5.365	0.093	0.0736	0.0014	0.1862	0.0032	1.870	0.049	0.0728	0.0015	0.656	1101	19	1009	40 −9
17.1	116	52	0.45	20	0.000018	0.03	4.898	0.069	0.0779	0.0010	0.2041	0.0029	2.186	0.045	0.0777	0.0011	0.693	1197	15	1138	29 −5
18.1	161	65	0.41	31	0.000071	0.12	4.481	0.059	0.0824	0.0012	0.2229	0.0029	2.501	0.053	0.0814	0.0013	0.627	1297	16	1230	32 −5
19.1	143	65	0.45	23	0.000079	0.13	5.355	0.073	0.0748	0.0010	0.1868	0.0026	1.934	0.036	0.0751	0.0010	0.733	1104	15	1071	26 −3
20.1	491	245	0.50	74	0.000032	0.05	5.730	0.068	0.0756	0.0005	0.1744	0.0021	1.807	0.026	0.0751	0.0006	0.842	1036	11	1072	15 3
21.1	53	36	0.68	8	0.000274	0.47	5.548	0.123	0.0762	0.0017	0.1794	0.0040	1.789	0.059	0.0723	0.0018	0.673	1064	22	995	49 −7
22.1	102	32	0.31	15	–	<0.01	5.660	0.086	0.0745	0.0012	0.1770	0.0027	1.854	0.050	0.0760	0.0017	0.566	1051	15	1094	44 4
23.1	134	74	0.55	21	0.000078	0.13	5.578	0.092	0.0773	0.0011	0.1791	0.0030	1.882	0.042	0.0762	0.0012	0.734	1062	16	1101	31 4
24.1	154	147	0.96	25	–	<0.01	5.307	0.083	0.0773	0.0010	0.1884	0.0029	2.009	0.041	0.0773	0.0010	0.765	1113	16	1130	26 1

(continued on next page)

Table 1 (*continued*)

Grain. spot	U (ppm)	Th (ppm)	Th/U	Pb* (ppm)	$^{204}Pb/^{206}Pb$	f_{206}%	Total ratios				Radiogenic ratios						ρ	Age (Ma)				
							$^{238}U/^{206}Pb$	±	$^{207}Pb/^{206}Pb$	±	$^{206}Pb/^{238}U$	±	$^{207}Pb/^{235}U$	±	$^{207}Pb/^{206}Pb$	±		$^{206}Pb/^{238}U$	±	$^{207}Pb/^{206}Pb$	±	%Disc
a) MAZ11043																						
25.1	265	192	0.73	49	0.000025	0.04	4.665	0.055	0.0808	0.0007	0.2143	0.0025	2.377	0.034	0.0804	0.0007	0.823	1252	13	1208	16	−4
26.1	170	184	1.08	21	0.000067	0.11	7.042	0.108	0.0741	0.0010	0.1418	0.0022	1.431	0.031	0.0732	0.0011	0.717	855	12	1019	30	16
27.1	215	126	0.59	38	–	<0.01	4.897	0.064	0.0835	0.0009	0.2042	0.0027	2.355	0.040	0.0836	0.0009	0.772	1198	14	1284	21	7
28.1	202	80	0.40	59	–	<0.01	2.927	0.038	0.1149	0.0009	0.3417	0.0044	5.415	0.082	0.1149	0.0009	0.856	1895	21	1879	14	−1
29.1	461	177	0.38	68	0.000134	0.22	5.808	0.067	0.0813	0.0006	0.1718	0.0020	1.880	0.030	0.0794	0.0009	0.727	1022	11	1181	21	13
30.1	261	66	0.25	42	0.000088	0.15	5.322	0.067	0.0770	0.0008	0.1878	0.0024	1.978	0.032	0.0764	0.0008	0.769	1109	13	1106	21	0
31.1	123	84	0.68	22	0.000107	0.18	4.715	0.072	0.0836	0.0012	0.2117	0.0032	2.396	0.052	0.0821	0.0013	0.704	1238	17	1247	30	1
32.1	144	119	0.82	41	–	<0.01	3.013	0.042	0.1157	0.0011	0.3319	0.0047	5.293	0.089	0.1157	0.0011	0.835	1848	23	1890	17	2
33.1	228	156	0.69	46	–	<0.01	4.265	0.055	0.0878	0.0009	0.2345	0.0030	2.840	0.046	0.0878	0.0009	0.800	1358	16	1379	19	2
34.1	30	25	0.83	9	–	<<0.01	2.964	0.071	0.1139	0.0024	0.3376	0.0081	5.330	0.171	0.1145	0.0025	0.745	1875	39	1872	39	0
35.1	82	54	0.66	24	–	<0.01	2.927	0.047	0.1187	0.0014	0.3416	0.0055	5.591	0.112	0.1187	0.0014	0.802	1895	26	1937	21	2
36.1	211	81	0.38	33	–	<0.01	5.512	0.074	0.0759	0.0009	0.1814	0.0024	1.900	0.034	0.0759	0.0009	0.740	1075	13	1093	24	2
37.1	104	67	0.64	17	0.000149	0.25	5.274	0.083	0.0766	0.0014	0.1892	0.0030	1.956	0.048	0.0750	0.0014	0.642	1117	18	1068	38	−5
38.1	314	160	0.51	134	–	<0.01	2.017	0.024	0.1782	0.0008	0.4957	0.0058	12.180	0.153	0.1782	0.0008	0.938	2595	25	2636	7	2
39.1	261	89	0.34	48	–	<0.01	4.699	0.064	0.0841	0.0013	0.2129	0.0029	2.480	0.052	0.0845	0.0013	0.657	1244	16	1304	31	5
40.1	407	276	0.68	65	0.000036	0.06	5.409	0.061	0.0759	0.0006	0.1848	0.0021	1.920	0.026	0.0753	0.0006	0.832	1093	11	1078	15	−1
41.1	109	63	0.57	18	0.000121	0.20	5.348	0.095	0.0784	0.0013	0.1866	0.0033	1.974	0.051	0.0767	0.0014	0.693	1103	18	1114	37	1
42.1	81	73	0.90	38	0.000075	0.10	1.830	0.029	0.2044	0.0016	0.5459	0.0086	15.323	0.269	0.2036	0.0016	0.895	2808	36	2855	13	2
43.1	129	71	0.55	22	0.000076	0.13	5.135	0.076	0.0783	0.0011	0.1945	0.0029	2.072	0.046	0.0773	0.0013	0.669	1146	15	1128	33	−2
44.1	160	85	0.53	32	0.000026	0.04	4.334	0.060	0.0870	0.0010	0.2306	0.0032	2.754	0.050	0.0866	0.0010	0.766	1338	17	1352	22	1
45.1	81	47	0.58	13	0.000140	0.24	5.278	0.088	0.0787	0.0014	0.1890	0.0032	1.999	0.058	0.0767	0.0018	0.570	1116	17	1114	48	0
46.1	135	121	0.90	35	0.000048	0.08	3.321	0.052	0.1059	0.0011	0.3009	0.0047	4.368	0.082	0.1053	0.0011	0.839	1696	24	1719	19	1
47.1	578	3	0.00	103	0.000019	0.03	4.823	0.057	0.0799	0.0005	0.2073	0.0024	2.277	0.031	0.0797	0.0005	0.864	1214	13	1189	14	−2
48.1	160	131	0.82	30	0.000130	0.22	4.573	0.063	0.0824	0.0010	0.2182	0.0030	2.422	0.050	0.0805	0.0013	0.665	1272	16	1210	31	−5
49.1	54	35	0.66	8	0.000136	0.23	5.540	0.124	0.0733	0.0016	0.1801	0.0041	1.771	0.089	0.0713	0.0032	0.449	1067	22	967	92	−10
50.1	110	73	0.67	32	0.000049	0.08	2.998	0.043	0.1132	0.0011	0.3333	0.0048	5.172	0.091	0.1126	0.0011	0.821	1854	23	1841	18	−1
51.1	77	41	0.53	15	0.000091	0.15	4.334	0.073	0.0885	0.0014	0.2304	0.0039	2.770	0.069	0.0872	0.0016	0.678	1336	20	1365	35	2
52.1	39	29	0.75	6	0.000110	0.19	5.417	0.119	0.0764	0.0020	0.1843	0.0041	1.902	0.094	0.0749	0.0033	0.449	1090	22	1065	89	−2
53.1	413	230	0.56	67	–	<0.01	5.309	0.063	0.0749	0.0006	0.1884	0.0022	1.944	0.028	0.0749	0.0006	0.815	1112	12	1065	17	−4
54.1	65	29	0.45	11	0.000078	0.13	5.336	0.098	0.0767	0.0016	0.1872	0.0034	1.951	0.056	0.0756	0.0017	0.635	1106	19	1085	45	−2
55.1	4	1	0.25	1	0.002497	4.16	4.163	0.245	0.1164	0.0069	0.2302	0.0144	2.578	0.666	0.0812	0.0204	0.243	1336	76	1227	492	−9
56.1	21	13	0.61	3	–	<0.01	5.473	0.156	0.0808	0.0028	0.1827	0.0052	2.035	0.092	0.0808	0.0028	0.629	1082	28	1216	69	11
57.1	77	45	0.58	12	0.000177	0.30	5.484	0.097	0.0765	0.0015	0.1818	0.0032	1.853	0.052	0.0739	0.0016	0.634	1077	18	1040	44	−4
58.1	34	21	0.62	7	–	<0.01	4.427	0.104	0.0849	0.0022	0.2259	0.0053	2.645	0.092	0.0849	0.0022	0.676	1313	28	1314	50	0
59.1	27	25	0.96	4	–	<0.01	5.102	0.136	0.0810	0.0026	0.1970	0.0053	2.314	0.143	0.0852	0.0047	0.438	1159	29	1320	107	12
60.1	190	49		30	0.000068	0.12	5.401	0.083	0.0753	0.0010	0.1849	0.0028	1.895	0.039	0.0743	0.0011	0.734	1094	15	1050	28	−4
61.1	230	68	0.30	37	–	<0.01	5.334	0.067	0.0750	0.0008	0.1875	0.0024	1.939	0.032	0.0750	0.0008	0.772	1108	13	1068	21	−4

Notes

1. Uncertainties given at the 1σ level.
2. Error in FC1 Reference zircon calibration was 1.01% for the analytical session, (not included in above errors but required when comparing $^{206}Pb/^{238}U$ data from different mounts).
3. f_{206} % denotes the percentage of ^{206}Pb that is common Pb.
4. Correction for common Pb made using the measured $^{204}Pb/^{206}Pb$ ratio.
5. For % Disc., 0% denotes a concordant analysis.

2005b) and ortho-amphibolites. The third domain (Western Domain) crops out in the western Sierra de Maz. It is a large fold anticline formed by two low-grade metasedimentary successions. The structurally upper succession consists of thick marble beds, Ca-pelitic schist, and quartzites (also assigned to the El Taco Group; Kilmurray and Dalla Salda, 1971), and is lithologically equivalent to the Difunta Correa sedimentary sequence of Sierra de Pie de Palo, a Neoproterozoic cover sequence to a Grenvillian basement (Varela et al., 2001; Casquet et al., 2001; Galindo et al., 2004). The structurally lower succession of Fe-rich garnet–chlorite schists with few quartzites (El Zaino Group; Kilmurray and Dalla Salda, 1971) is of unknown age.

The anorthosites and their host rocks were overprinted by a Famatinian garnet–amphibolite facies metamorphism at c. 430 Ma (Casquet et al., 2005a). High-grade metamorphism of the Eastern Domain was also dated (U–Pb SHRIMP zircon) at 452±6 Ma (Casquet et al., 2001). It is most likely that the whole area underwent Famatinian metamorphism and deformation (see also Lucassen and Becchio, 2003).

4. Sampling and analytical methods

Detrital zircon U–Pb ages from two metasedimentary rocks from the Eastern and Western Domains respectively are presented here to constrain their depositional ages and to compare with those of the Grenvillian-age Maz Domain (Casquet et al., 2006). RAM-1013 (Fig. 1) is an amphibolite facies garnet–scapolite–clinopyroxene calc-silicate gneiss from the El Taco metasedimentary sequence (Kilmurray and Dalla Salda, 1971) from the Sierra de las Ramaditas (Fig. 1), in the Eastern Domain. Sample MAZ-11043 (Fig. 1) is a greenschist facies chlorite–garnet schist from the El Zaino Group in the Western Domain.

Zircon separates were prepared using Rogers table, superpanner, Frantz isodynamic separator and di-iodomethane at NERC Isotope Geosciences Laboratory, UK (sample RAM-1013) and bromoform followed by di-iodomethane and Frantz isodynamic separator at RSES, Canberra (sample MAZ-11043). Resin mounts were made, polished and analysed using SHRIMP II and SHRIMP RG at RSES. Analytical results are presented in Table 1. Cathodo-luminescence (CL) images, relative probability plots and Concordia diagrams are shown in Fig. 2.

Because Nd and Sm, and Pb isotopes do not fractionate significantly during metamorphism and erosion (e.g., Faure, 1986; DePaolo, 1988; Nelson and DePaolo, 1988), Nd and Pb isotope composition of metasedimentary rocks constitute a valuable tool for distinguishing provenance, i.e., source regions with a characteristic average isotope composition at the time of sedimentation. They are modelled to record when Nd was first extracted from the mantle into the continental crust. Pb isotopes allow distinction between large scale reservoirs (e.g., mantle or continental crust) (Gariépy and Dupre, 1991). Nd and Pb isotope compositions of sedimentary rocks might thus be useful to distinguish continental crustal provinces in the sense of DePaolo (1988), and thus for the correlation of separated crustal domains.

Twenty four samples of metasedimentary rocks (metasandstones and metapelites) were collected. They are from: (1) the Maz Domain (Grenvillian) in Sierra de Maz (10 samples), (2) the Eastern Domain, including eastern Sierra del Espinal (2 samples), the nearby Villa Castelli massif (3 samples) and the El Taco Group at Ramaditas (3 samples), and (3) the Western Domain El Zaino sequence (3 samples) and the El Taco Group (2 samples). Five metasedimentary samples from Sierra de Pie de Palo (the Difunta Correa sedimentary sequence) were added for comparison. All these samples were analysed for Sm and Nd, and sixteen were analysed for Pb-isotope composition. Sample identification, lithological name, location and analytical results are given in Table 2 and in Figs. 1, 3 and 4). The Sm–Nd analytical method was as described by Galindo et al. (1994). Analytical errors (2σ) are 0.2% and 0.006% for the $^{147}Sm/^{144}Nd$ and $^{143}Nd/^{144}Nd$ ratios, respectively. Common Pb was analysed following the method of Chiaridia and Fontboté (2003). For each sample, the method provides separate lead isotope analysis of acid ($HCl+HNO_3$) leachate and residue fractions. The leachate contains radiogenic and common Pb derived from labile sites in silicate minerals and secondary minerals, which are easily dissolved in the acid solution. The residue Pb isotope composition of medium- to high-grade rocks corresponds for the most part to feldspar-hosted common Pb, i.e., the original Pb contained in the sediment, for which an age correction is unnecessary. The contribution to the whole-rock Pb isotope composition of radiogenic Pb from zircon retained in the residue is comparatively very small. However, in the low-grade metamorphic rocks that lack feldspars, most of the common Pb is lost in the leachate, which is thus less radiogenic than the residua, the latter swamped by radiogenic lead of detrital zircons (Chiaridia and Fontboté, 2003). In our samples residues were always less radiogenic than leachates irrespective of metamorphic grade. Pb isotope results for the residues are listed in Table 2, along with the corresponding model $^{238}U/^{204}Pb$ (μ) values calculated with ISOPLOT (Ludwig, 1999).

5. U–Pb SHRIMP results

Zircons from RAM-1013 are subhedral oval to elongate, up to 300 μm in length and mostly clear and colourless. Cathodo-luminescence images (Fig. 2a) show that the shape is dictated by medium-luminescence overgrowths that mostly envelope each grain; cores are irregular and variable but mostly show evidence of oscillatory zoning. MAZ-11043 zircons are smaller (generally 100 μm), anhedral but angular in form, and show a predominance of simple or oscillatory zoning under cathodo-luminescence.

RAM-1013 zircons were analysed first on SHRIMP II, with subsequent additional rim analyses on SHRIMP RG in geochronology mode. The results (Table 1, Fig. 2) display a marked difference between the overgrowths, which have $^{238}U–^{206}Pb$ ages less than 600 Ma, and the cores, with ages of more than 1000 Ma. In detail, most of the rim ages fall in the range 425 to 465 Ma, and the weighted mean for 28 out of 32 of these is 442±3 Ma (MSWD=1.8). All of these have relatively low Th/U ratios (0.1–0.4) consistent with a metamorphic origin for the overgrowths. A small group of four rims have ages in the range 570–500 Ma, which could be explained as partial inheritance from older core material. The core ages (calculated from $^{207}Pb/^{206}Pb$) range from 1000 Ma to 1440 Ma, with one slightly discordant va`lue at

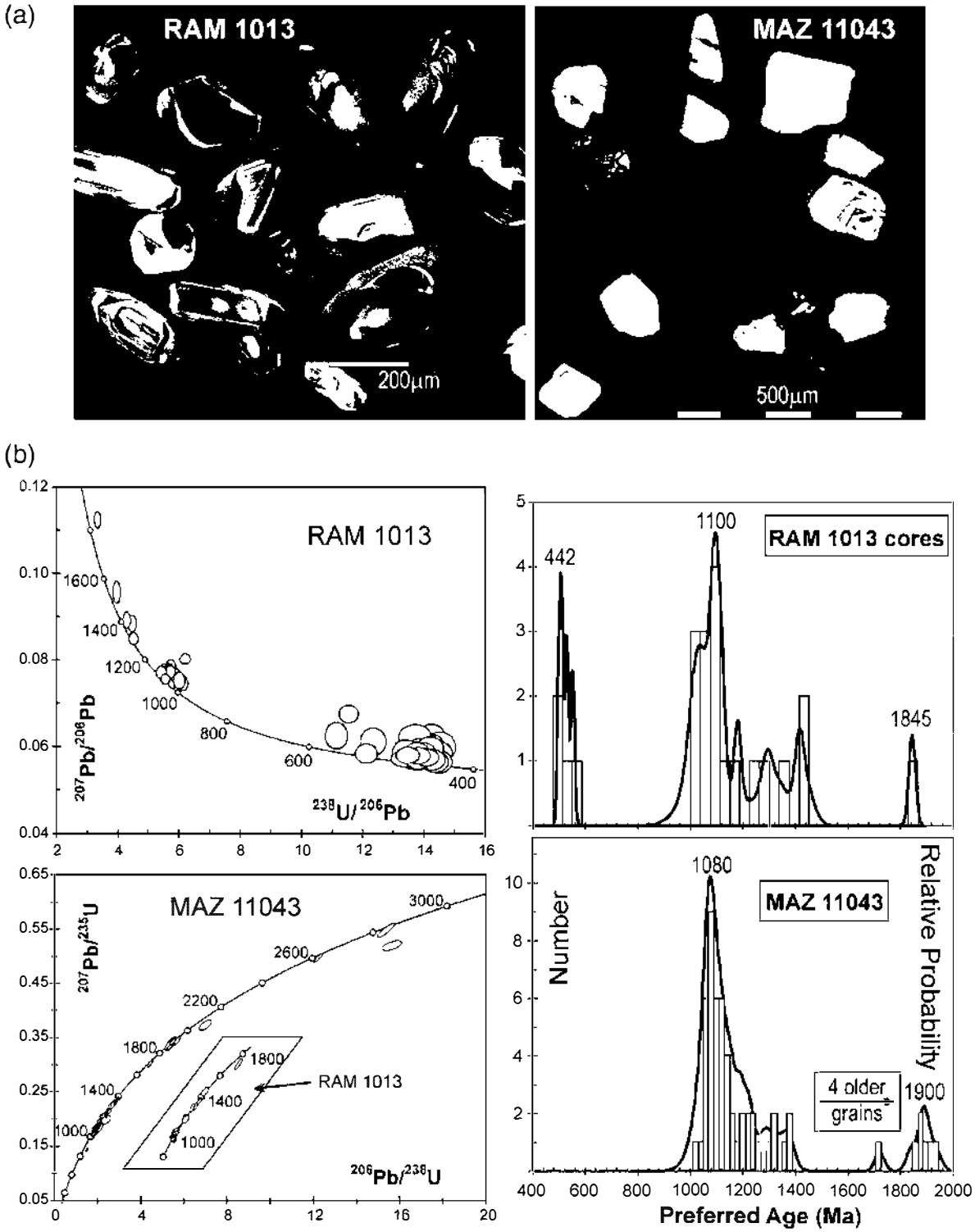

Fig. 2. U–Pb SHRIMP zircon geochronology of samples RAM-1013 and MAZ-11043. (a) Typical cathodo-luminescence images; that for RAM-1013 shows broad (up to 50 μm) unzoned metamorphic rims overgrowing a wide variety of fragmental cores, whereas MAZ-11043 lacks these overgrowths. (b) Concordia plots and probability density plots for the derived ages for the two samples — the best defined provenance is at 1000–1050 Ma in both cases, but RAM-1013 also shows an Ordovician peak defined by the rim data (white error ellipses in Tera–Wasserburg plot).

1845 Ma, but with a bias to the younger end of the range; a significant peak in the distribution occurs at 1100 Ma. This is interpreted as representing a major 'Grenville-age' igneous event in the source area of the sample.

The data for MAZ-11043, analysed on SHRIMP RG in provenance (four-scan) mode, show no evidence of Phanerozoic ages. There is a predominant spread of concordant ^{207}Pb–^{206}Pb ages in the range 1040–1380 Ma, with a small secondary peak

Table 2
Sm–Nd and Pb isotope data for metasedimentary rocks from the Western Sierras Pampeanas

Sample	Rocks	Latitude S	Longitude W	Sm ppm	Nd ppm	Sm/Nd	$^{147}Sm/^{144}Nd$	$^{143}Nd/^{144}Nd$	T_{DM} Ga	$^{206}Pb/^{204}Pb$	$^{207}Pb/^{204}Pb$	$^{208}Pb/^{204}Pb$	μ
Western Domain — El Zaino Group													
MAZ-6036	Quartzite	29°11′20.1	68°28′49.6	19.6	82.9	0.2364	0.1429	0.512374	1.4				
MAZ-7218	Quartzite	29°11′29.9	68°29′43.6	7.08	32.70	0.2165	0.1309	0.512162	1.6	18.141	15.585	37.815	9.68
MAZ-11030	Quartzite	29°10′43.7	68°29′11.2	9.93	45.70	0.2173	0.1314	0.512286	1.4	18.118	15.599	37.887	9.75
MAZ-7217	Grt-Chl schist	29°11′29.9	68°29′43.6	4.22	20.94	0.2015	0.1218	0.512133	1.5	18.153	15.593	37.873	9.71
MAZ-11044	Chl-Grt schist	29°03′56.2	68°24′43	5.63	31.80	0.1770	0.1070	0.512108	1.3				
Western Domain — El Taco Group													
MAZ-11012	Calcic metapelite	29°27′59.7	68°29′30.3	4.69	23.22	0.2020	0.1221	0.512241	1.3				
MAZ-11013	Calcic metapelite	29°27′59.7	68°29′30.3	8.24	42.00	0.1962	0.1186	0.512092	1.5				
Maz Domain (Grenvillian)													
MAZ-7219	Ms-chl schist (retrograde)	29°11′10.4	68°27′24	10.41	56.83	0.1832	0.1107	0.511502	2.3	21.050	16.043	42.746	11.11
MAZ-7220	St-Ms-Grt schist	29°11′10.4	68°27′24	6.44	36.05	0.1786	0.1080	0.511452	2.3	17.585	15.659	37.761	10.23
MAZ-11032	St-Ms-Grt schist	29°11′10	68°27′24	6.93	39.36	0.1760	0.1064	0.511422	2.3				
MAZ-11005	Hb+Bt gneiss	29°14′36	68°21′34.3	6.45	43.10	0.1497	0.0904	0.511531	1.9	18.034	15.614	41.165	9.84
MAZ-7223	Grt-schist	29°11′35.2	68°24′27.2	4.16	25.08	0.1659	0.1003	0.511469	2.1	18.063	15.684	38.722	10.16
MAZ-11034	Grt schist	29°11′33	68°24′31	7.40	39.32	0.1881	0.1137	0.511576	2.2				
MAZ-11035	Grt schist	29°11′24.3	68°23′45.9	3.52	17.97	0.1956	0.1182	0.511971	1.7				
MAZ-11062	Grt gneiss	29°16′07.7	68°20′57	2.66	12.90	0.2062	0.1246	0.511834	2.1	17.868	15.620	37.989	9.92
MAZ-11063	Quartzite	29°16′09.1	68°20′41.3	3.02	18.00	0.1678	0.1014	0.511077	2.7				
Eastern Domain													
Ramaditas–El Taco Group													
RAM-1013	Calc silicate rock	29°14′07.7	68°15′34.4	7.00	31.57	0.2218	0.1341	0.512265	1.5				
RAM-11017	Grt-Sill migmatite	29°17′51.7	68°17′48.9	4.87	26.64	0.1829	0.1105	0.512029	1.5	18.245	15.585	37.937	9.65
RAM-11021	Grt-Sill migmatite	29°18′02.1	68°19′22.2	8.44	42.42	0.1990	0.1203	0.512314	1.2	18.206	15.568	37.839	9.59
Eastern Espinal													
ESP-11045	Grt+Sill migmatite	29°03′36	68°26′10	10.79	58.62	0.1840	0.1112	0.512003	1.5	18.232	15.631	38.126	9.86
ESP-11053	Grt+Sill migmatite	29°03′56.2	68°24′43	4.90	26.50	0.1849	0.1118	0.512082	1.4	18.259	15.624	38.064	9.82
Villa Castelli													
VCA-1004	Grt-Sill migmatite	28°59′11.4	68°16′01.1	7.62	39.29	0.1938	0.1172	0.512034	1.6				
VCA-7224	Grt-Sill migmatite	28°59′06.5	68°16′40.5	9.77	52.37	0.1866	0.1128	0.512039	1.5	18.568	15.670	38.718	9.95
VCA-7225	Grt-Sill migmatite	28°59′11.4	68°16′01.1	7.00	37.54	0.1865	0.1127	0.512088	1.4	18.368	15.674	38.299	10.02
Sierra de Pié de Palo–Difunta Correa Sedimentary Sequence													
PPL-15A	Calcic metapelite	31°42′22	68°05′43	7.80	35.00	0.2229	0.1347	0.512198	1.5	18.354	15.531	37.830	9.39
PPL-23	Calcic metapelite	31°42′55	68°05′42	7.75	39.22	0.1976	0.1194	0.512192	1.4	18.569	15.567	37.984	9.50
SPP-1001	Calcic metapelite	31°42′22	68°05′43	7.15	34.07	0.2097	0.1268	0.512238	1.4				
SPP-424	Grt schist	31°22′ 55	67°58′42	13.05	64.30	0.2030	0.1227	0.512384	1.1				
SPP-6086	Meta-conglomerate	31°43′0.8	68°05′48.5	1.08	6.05	0.1785	0.1079	0.512099	1.5				

at 1900 Ma and a few scattered older ages to almost 3000 Ma. The skew in the 'Grenville-age' group is more marked than for RAM-1013, with possible resolved components at 1080 Ma (80%) and 1165 Ma (20%).

The main differences in these two patterns are the Ordovician ages for the overgrowths of RAM-1013, the 500–570 Ma group in the same sample (although these could be mixed age), and the oldest components in MAZ-11043. The main provenance ages of c. 1000 to 1400 Ma and c. 1900 Ma are better defined in the latter, low-grade, rock, but are also identifiable in RAM-1013.

6. Nd and Pb isotope results

Nd isotope results are best represented as depleted mantle model ages (T_{DM}). Logically, for reworked crustal material such as these metasedimentary rocks, the multi-stage model of DePaolo et al. (1992) should be used, but for simplicity of comparison with other data, the single stage model ages have been calculated according to the quadratic curve for the evolution of Nd in the mantle (DePaolo, 1981) (Table 1). Both T_{DM} values are shown in Table 2, and it can be seen that the multistage values are older, generally by up to 200 Ma. Single stage T_{DM} ages are plotted together with published data for the Arequipa–Antofalla terrane in Fig. 3.

Nd T_{DM} model ages for the northern WSP, i.e., Sierra de Maz, Sierra del Espinal, Ramaditas and Villa Castelli range from 1.2 to 2.7 Ga, with a main cluster between 1.2 and 1.6 Ga (Mesoproterozoic) peaking at c. 1.4 Ga, and a smaller cluster between 1.7 and 2.7 Ga (Paleoproterozoic) peaking at c. 2.2 Ga (Fig. 3). Ages younger than 1.2 Ga have not been recorded from these areas. The two T_{DM} peaks correspond respectively to the geological domains formerly distinguished on the basis of metamorphic and lithological considerations (see above). The Paleoproterozoic ages (above c. 1.7) are exclusive to the Maz Domain, whilst the Mesoproterozoic ages are restricted to the Eastern and Western Domains (see also Porcher et al., 2004). Significantly, the lower

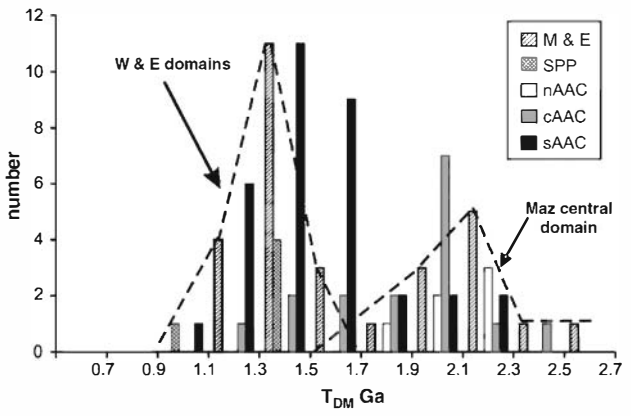

Fig. 3. Histogram of single-stage Nd (T_{DM}) model ages of metasedimentary rocks from Maz and Espinal region, including those of Porcher et al. (2004), and from the Sierra de Pie de Palo (Table 2). Added for comparison are Nd model ages of metasedimentary rocks from the Arequipa–Antofalla craton (Bock et al., 2000; Loewy et al., 2004). Division of the Arequipa–Antofalla craton is after Loewy et al. (2004): nAAC = northern; cAAC = central; sAAC = southern.

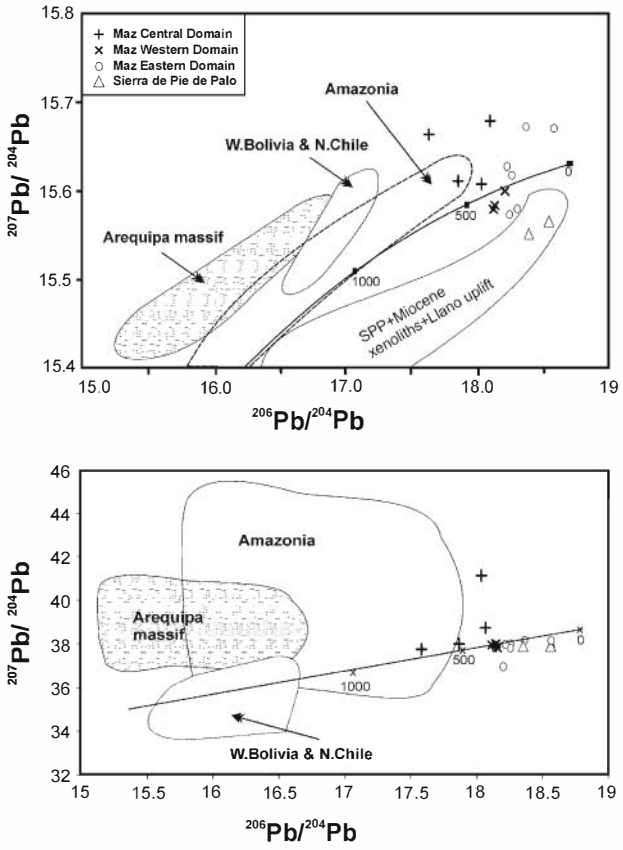

Fig. 4. $^{207}Pb/^{206}Pb$ vs. $^{206}Pb/^{204}Pb$ and $^{208}Pb/^{206}Pb$ vs. $^{206}Pb/^{204}Pb$ plots of residues of samples of metasedimentary rocks from the Maz and Espinal region and the Sierra de Pie de Palo (Table 2). Added for comparison are age-corrected Pb compositions of the Arequipa massif (Barreiro, 1982, *in* Tosdal, 1996), W Bolivia and Northern Chile (Tosdal, 1996) and Amazonia (Tosdal and Bettencourt, 1994, *in* Tosdal, 1996). $^{208}Pb/^{206}Pb$ values of Arequipa massif and Amazonia are present-day values. Also shown is the crustal Pb-growth curve of Stacey and Kramers (1975).

T_{DM} values are also recorded from the Sierra de Pie de Palo (T_{DM} 1.1 to 1.5 Ga).

Pb isotope composition of the residues (Table 2) was plotted in uranogenic $^{207}Pb/^{204}Pb$ vs. $^{206}Pb/^{204}Pb$ and thorogenic $^{208}Pb/^{204}Pb$ vs. $^{206}Pb/^{204}Pb$ diagrams (Fig. 4a and b, respectively). The Stacey and Kramers (1975) Pb-isotope crustal growth curve from ISOPLOT (Ludwig, 1999) is added for reference. In Fig. 4a our data lie above and below the crustal growth curve. Those below are from the Western Domain El Zaino Group and from the Ramaditas El Taco Group. The two samples from the Sierra de Pie de Palo Difunta Correa sedimentary sequence plot well below the crustal growth curve. The rest of the samples (Maz Domain, eastern Espinal and Villa Castelli) plot above the crustal growth curve. Sample MAZ-7219 is highly radiogenic, probably because the leachate failed to remove all radiogenic lead and this datum will not be considered further. Taken together all the metasedimentary rocks show high $^{206}Pb/^{204}Pb$ values (17.58–18.57). The relatively high $^{207}Pb/^{204}Pb$ (15.6–16.0) of those metasedimentary rocks that lie above the crustal growth curve suggests that Pb was derived from reworking of a pre-Grenvillian, probably Paleoproterozoic (or even Archean) continental crust, in agreement with the high model μ values (up to 10.23) (Wareham et al., 1998).

However rocks that plot below the crustal growth curve do not support a significant pre-Grenvillian continental crust Pb component. In Fig. 4b only the data from the Maz Domain plot above the crustal growth curve; all others lie on or below the reference curve and do not depart significantly from it.

7. Interpretation and discussion

U–Pb SHRIMP ages of zircons from the Ramaditas El Taco Group calc-silicate rocks and the El Zaino schist suggest that both the Eastern and Western Domains consist of metasedimentary rocks with depositional ages younger than c. 1.0 Ga, i.e., Neoproterozoic and/or Early Paleozoic. Moreover both samples have detrital zircon age patterns remarkably similar to those of the Late Neoproterozoic Difunta Correa sedimentary sequence from Sierra de Pie de Palo (Casquet et al., 2001; Rapela et al., 2005). Provenance ages in this group of samples range from c. 1.0 to c. 1.5 Ga with a main peak at c. 1.1 (Grenvillian) and a secondary one at c. 1.4 Ga, except for a few Gondwana detrital zircons of c. 625 Ma found in the Difunta Correa rocks (Rapela et al., 2005) and the few Paleoproterozoic and Archean zircons found in our samples. The age of the Difunta Correa Sedimentary Sequence was constrained between a maximum of c. 625 Ma (from detrital zircons) and a minimum of c. 580 Ma (Sr isotope dating of marine carbonates; Galindo et al., 2004). The age of El Zaino Group however remains unknown so far. Most zircons in the El Zaino schist and the El Taco Group calc-silicate rocks were derived from a Grenville-age igneous source. Grenville-age igneous rocks (1.0 and 1.2 Ga) have been recognized in the nearby Maz Domain and in the Sierra de Pie de Palo (McDonough et al., 1993; Pankhurst and Rapela, 1998). The source of the older zircons remains speculative (for a discussion see Rapela et al., 2005). Detrital zircons of one garnet schist from the eastern part of the Maz Domain, that underwent granulite facies metamorphism at c. 1.2 Ga, have apparent peaks at c. 1.7 and 1.9 Ga (Casquet et al., 2006). The source of these Paleoproterozoic zircons might well have been the same as for the El Zaino and El Taco Group Paleoproterozoic zircons. Casquet et al. (2006) suggested that this source might be found in the Paleoproterozoic igneous complex of the northern Arequipa–Antofalla craton.

Nd and Pb isotopic evidence from metasedimentary rocks confirms that the Maz Domain on one hand and the Eastern and Western Domains are different. Because of the high Nd T_{DM} values (1.7–2.7 Ga) and of the highly uranogenic Pb-isotope compositions, the Maz Domain sedimentary protoliths were probably derived from an old continental source area mainly formed in the Early Paleoproterozoic (c. 2.5 Ga or older), and reworked with significant juvenile accretion in the Late Paleoproterozoic. Minor additions from an older crustal, i.e., Archean, component are difficult to recognize although might be expected from the high $^{207}Pb/^{204}Pb$ values (Wareham et al., 1998). Sedimentary protoliths in the Eastern and Western Domains however incorporated predominantly younger juvenile Nd (T_{DM} between 1.2 and 1.6 Ga) that was added to the crust in the Mesoproterozoic, in part during the Grenvillian orogeny (1.0–1.2 Ga). In fact, the Grenvillian massif-type anorthosites of c. 1.1 Ga contain significant juvenile Nd (T_{DM} model ages between 1.2 and 1.5 Ga; Casquet et al., 2005a,b). Moreover this evidence is consistent with the detrital zircon ages, which suggest a significant input from a Grenvillian igneous source. Significantly, the lowest T_{DM} value (1.1 Ga) is recorded from the Sierra de Pie de Palo where an ophiolite complex of Grenvillian age has been recognized (1.1 to 1.2 Ga; Vujovich and Kay, 1998; Vujovich et al., 2004). The range of Nd T_{DM} ages for Sierra de Pie de Palo (1.1 to 1.5 Ga), is largely coincident with that recorded from inherited zircon ages (Casquet et al., 2001) and with the ophiolite age, suggesting that a juvenile crustal component of 1.1–1.2 Ga, and a slightly older continental crust component (T_{DM} age up to c. 1.5 Ga) were involved in the sedimentary protoliths in this sierra.

Pb isotope compositions of post-Grenvillian metasedimentary sequences allow further discrimination between them. On one hand, eastern Espinal and Villa Castelli migmatitic gneisses have Pb isotope compositions well above the crustal growth curve in uranogenic space with high μ values (9.82–10.02) suggesting that Pb was originally derived from the same source as the Maz Domain pre-Grenvillian metasedimentary rocks. The shift toward higher $^{206}Pb/^{204}Pb$ values shown by these samples probably reflects radiogenic Pb growth between the Mesoproterozoic and the age of sedimentation, i.e., Neoproterozoic or early Paleozoic. On the other hand metasedimentary rocks from the El Taco Group (Ramaditas) and El Zaino Group (Western Domain) plot below the crustal growth curve implying a significant Pb contribution from a U-depleted source. This source might be found in a crust equivalent to the Grenvillian Sierra de Pie de Palo and Precordillera basement domain. This crust is isotopically similar to that of the Grenville belt of North America and formed in an oceanic-arc or back-arc environment (ay et al., 1996; Vujovich et al., 2004). Mixing of this juvenile component with a radiogenic continental crust component might explain why these rocks lie between those of the Maz Domain and those of Sierra de Pie de Palo and Precordillera basement in both uranogenic and thorogenic plots. Nd and Pb isotope evidence thus suggest that at least three post-Grenvillian and pre-Famatinian metamorphism metasedimentary sequences exist in this region: the eastern Espinal and Villa Castelli migmatitic gneisses of unknown age, the El Taco Group of probable late Neoproterozoic age (630–580 Ma), and the El Zaino Group of unknown age.

It is interesting at this point to compare Pb and Nd isotope compositions from the Western Sierras Pampeanas with those of other Grenville-age and older regions, particularly with the Arequipa–Antofalla block in the north and the large Amazonia craton in the northeast. Nd data are from Bock et al. (2000) and Loewy et al. (2003, 2004) and refer to metasedimentary rocks only (Fig. 3). Pb data are from Tosdal (1996 and references therein) (Fig. 4). Also added for comparison are Pb isotope compositions of Grenvillian rocks from the El Llano Uplift (Texas), i.e., the Appalachian margin of Laurentia (Roback et al., 1995), the Argentina Precordillera present-day basement (xenoliths in Tertiary volcanics; Abruzzi et al., 1993) and the Sierra de Pie de Palo ophiolite (ay et al., 1996). T_{DM} ages of the Arequipa–Antofalla craton metasedimentary rocks clearly young southward (Loewy et al., 2004) (Fig. 3). Those of the

northern part of the craton, i.e., from the Arequipa massif, are coincident with those of the Maz Domain (between 1.7 and 2.6 Ga). Those of the central and southern parts of the craton however spread from c. 1.1 to 2.6 Ga, attesting to a mixing of Paleoproterozoic and juvenile Grenvillian sources. Moreover, the peak Nd T_{DM} ages of the southern Arequipa–Antofalla craton are ca. 1.4 Ga, i.e., similar to those of post-Grenvillian Western and Eastern Domains in the Maz–Espinal area. However Maz Domain samples have $^{206}Pb/^{204}Pb$ values higher than those of northern and central Arequipa–Antofalla craton (Tosdal, 1996 and references therein; craton division after Loewy et al., 2004) and lie close to the more radiogenic part of the Amazonia field (Tosdal, 1996, and references therein) in both uranogenic and thorogenic space (Fig. 4). This fact suggests that the old crustal source of the Maz Domain Pb might be found in the early Amazonia craton. A connection with this latter craton was also suggested for the northern and central Arequipa–Antofalla craton because of the high $^{207}Pb/^{204}Pb$ values. Amazonia in fact, is the nearest high $^{207}Pb/^{204}Pb$ craton (Tosdal, 1996). Moreover the Maz Domain samples lie along crustal growth curves passing through the Arequipa–Antofalla and Amazonia fields, suggesting that these domains share common original Pb sources.

We conclude that similarities and differences exist between the Northern and Central Arequipa–Antofalla craton, and the Maz Domain pre-Grenvillian metasedimentary rocks. Similarities include: (1) the coincident range of Nd model ages between 2.6 and 1.7 Ga, (2) the Paleoproterozoic detrital zircon ages found in the Maz Domain metasedimentary rocks that are compatible with a igneous source of c. 1.8–1.9 Ga, similar to the age of northern Arequipa–Antofalla craton orthogneisses, and (3) the presence in both domains of a mobile belt of Grenvillian age (1.0–1.2 Ga) with granulite facies metamorphism and massif-type anorthosites (Casquet et al., 2006). Differences refer to the old crustal source of Pb. In both regions an early crust underwent reworking during the early Paleoproterozoic or the Archean to produce a new crust enriched in U relative to Pb. Why the resulting Pb isotope composition in the Mesoproterozoic resulted to be so different between the two areas might result from an older, pre-Grenvillian metamorphic event in Arequipa–Antofalla that led to U depletion and consequently retarded growth of the $^{206}Pb/^{204}Pb$ ratios. Evidence for a 1.7–1.9 Ga metamorphic event has been in fact suggested by (Shackleton et al., 1979).

The Arequipa–Antofalla pre-Grenvillian basement and the unexposed basement of the Maz Domain Mesoproterozoic metasedimentary rocks were once continuous along the paleo-margin of the Amazonia craton. During the Grenville orogeny the two regions were part of the same mobile belt and remained autochthonous to Western Gondwana at least until the end of the Neoproterozoic (Rapela et al., 2005; Ca quet et al., 2006). The relationships with the Sierra de Pie de Palo and the Precordillera basement domains in the south are unknown because of the Andean first order Desaguadero–Bermejo fault that separates both crustal areas. However the presence in the Maz and Espinal region of post-Grenvillian metasedimentary rocks with juvenile Nd and Pb signatures (El Taco and El Zaino Groups) is compatible with a juvenile Grenvillian source such as the Sierra de Pie de Palo and the Precordillera basement. In the latter hypothesis the two latter domains would be adjacent to the Maz Domain in Grenvillian times and would thus be representative of a Grenvillian suture that was autochthonous to western Gondwana at least until late Neoproterozoic times.

Western Sierras Pampeanas thus consists of a mosaic of geologic domains or terranes with different tectonothermal, sedimentary and igneous histories now separated by shear zones and younger faults. The Maz Domain can thus be considered a suspect terrane, i.e., the Maz terrane, that is remarkable because it contains the oldest evidence for the geologic history of the pre-Andean western Gondwana margin.

Acknowledgements

Financial support for this paper was provided by Spanish MEC grants BTE2001-1486 and CGL2005-02065/BTE, Universidad Complutense grant PR1/05-13291 and Argentine public grants (FONCYT PICT 07-10735; CONICET PIP 5719; CONICET PEI-6275). R.J.P. acknowledges a NERC Small Research Grant.

References

Abruzzi, J.M., Kay, S.M., Bickford, M.E., 1993. Implications for the nature of the Precordilleran basement from the geochemistry and age of Precambrian xenoliths in Miocene volcanic rocks, San Juan province. XII Congreso geológico Argentino y II Congreso de Exploración de Hidrocarburos, Mendoza, Actas III, pp. 331–339.

Astini, R.A., Benedetto, J.L., Vaccari, N.E., 1995. The early Paleozoic evolution of the Argentina Precordillera as a Laurentian rifted, drifted and collided terrane: a geodynamic model. Geological Society of American Bulletin 107, 253–273.

Baldo, E., Casquet, C., Pankhurst, R.J., Rapela, C.W., Galindo, C., Dahlquist, J., Murra, J., Fanning, C.M., 2006. Neoproterozoic A-type magmatism in the Western Sierras Pampeanas (Argentina): evidence for Rodinia break-up along a proto-Iapetus rift? Terra Nova 18, 388–394.

Benedetto, J.L., 1998. Early Palaeozoic brachiopods and associated shelly faunas from western Gondwana: their bearing on the geodynamic history of the pre-Andean margin. In: Pankhurst, R.J., Rapela, C.W. (Eds.), The Proto-Andean margin of South America. Geological Society of London, Special Publication, vol. 142, pp. 57–84.

Bock, B., Bahlburg, H., Wörner, G., Zimmerman, U., 2000. Tracing crustal evolution in the Southern Central Andes from Late Precambrian to Permian with geochemical and Nd and Pb data. Journal of Geology 108, 515–535.

Casquet, C., Baldo, E., Pankhurst, R.J., Rapela, C.W., Galindo, C., Fanning, C.M., Saavedra, J., 2001. Involvement of the Argentine Precordillera Terrane in the Famatinian mobile belt: geochronological (U–Pb SHRIMP) and metamorphic evidence from the Sierra de Pie de Palo. Geology 29, 703–706.

Casquet, C., Rapela, C.W., Pankhurst, R.J., Galindo, C., Dahlquist, J., Baldo, E.G., Saavedra, J., González Casado, J.M., Fanning, C.M., 2005a. Grenvillian massif-type anorthosites in the Sierras Pampeanas. Journal of the Geological Society of London 162, 9–12.

Casquet, C., Pankhurst, R.J., Rapela, C.W., Fannning, C.M., Galindo, C., Baldo, E., González-Casado, J.M., Dahlquist, J., Saavedra, J., 2005b. The Maz suspect terrane: a new Proterozoic domain in the Western Sierras Pampeanas. In: Pankhurst, R.J., Veiga, G.D. (Eds.), Gondwana 12: Geological and Biological Heritage of Gondwana, p. 92. Abstracts.

Casquet, C., Pankhurst, R.J., Fanning, C.M., Baldo, E., Galindo, C., Rapela, C., González-Casado, J.M., Dahlquist, J.A., 2006. U–Pb SHRIMP zircon dating of Grenvillian metamorphism in Western Sierras Pampeanas (Argentina): correlation with the Arequipa Antofalla craton and constraints on the extent of the Precordillera Terrane. Gondwana Research 9, 524–529.

Chiaridia, M., Fontboté, L., 2003. Separate lead isotope analyses of leachate and residue rock fractions: implications for metal source tracing in ore deposit studies. Mineralium Deposita 38, 185–195.

Dalla Salda, L., Cingolani, C., Varela, R., 1992. Early Paleozoic orogenic belt of the Andes in southwestern South America, result of Laurentia–Gondwana collision? Geology 20 (7), 617–620.

Damm, K.W., Pichowiak, S., Harmon, R.S., Todt, W., Kelley, S., Omarini, R., Niemeyer, H., 1990. Pre-Mesozoic evolution of the Central Andes, the basement revisited. Geological Society of America, Special. Paper. 241, 101–126.

DePaolo, D.J., 1981. Neodymium isotopes in the Colorado Front Range and crust–mantle evolution in the Proterozoic. Nature 291, 193–196.

DePaolo, D.J., 1988. Age dependence of the composition of continental crust, evidence from Nd isotopic variations in granitic rocks. Earth and Planetary Science Letters 94 (4), 382–394.

DePaolo, D.J., Perry, F.V., Baldridge, W.S., 1992. Crustal versus mantle sources of granitic magmas: a two-parameter model based on Nd isotopic studies. Earth Science Transactions of the Royal Society of Edinburgh 83, 439–446.

Faure, G., 1986. Principles of Isotope Geology. John Wiley & Sons, New York.

Galindo, C., Tornos, F., Darbyshire, D.P.F., Casquet, C., 1994. Sm/Nd dating and isotope constraints for the origin of the barite–fluorite (Pb–Zn) veins of the Sierra del Guadarrama (Spanish Central System, Spain). Chemical Geology 112, 351–364.

Galindo, C., Casquet, C., Rapela, C., Pankhurst, R.J., Baldo, E., Saavedra, J., 2004. Sr, C and O isotope geochemistry and stratigraphy of Precambrian and Lower Paleozoic carbonate sequences from the Western Sierras Pampeanas of Argentina: tectonic implications. Precambrian Research 131, 55–71.

Gariépy, C., Dupre, B., 1991. Pb isotopes and crust–mantle evolution. In: Heaman, L., Ludden, J.N. (Eds.), Mineralogical Association of Canada. Short Course Handbook on Application of Radiogenic Isotope Systems to Problems in Geology, vol. 19, pp. 191–224.

Kay, S.M., Orrell, S., Abruzzi, J.M., 1996. Zircon and whole-rock Nd–Pb isotopic evidence for a Grenville age and Laurentian origin for the basement of the Precordillera in Argentina. Journal of Geology 104, 637–648.

Kilmurray, J.O., Dalla Salda, L., 1971. Las fases de deformación y metamorfismo en la sierra de Maz, provincia de La Rioja, República Argentina. Revista de la Asociación Geológica Argentina 26 (2), 245–263.

Loewy, S.L., Connelly, J.N., Dalziel, I.W.D., Gower, C.F., 2003. Eastern Laurentia in Rodinia: constraints from whole-rock Pb and U/Pb geochronology. Tectonophysics 375, 169–197.

Loewy, S.L., Connelly, J.N., Dalziel, I.W.D., 2004. An orphaned basement block: the Arequipa–Antofalla Basement of the central Andean margin of South America. Geological Society of American Bulletin 116, 171–187.

Lucassen, F., Becchio, R., 2003. Timing of high-grade metamorphism: early Palaeozoic U–Pb formation ages of titanite indicate long-standing high-T conditions at the western margin of Gondwana (Argentina, 26–29 degrees S). Journal of Metamorphic Geology 21 (7), 649–662.

Ludwig, K., 1999. Isoplot/ex, a geochronological toolkit for Microsoft Excel. Special Publication, vol. 1. Berkeley Geochronological Center.

Martignole, J., Martelat, J.E., 2003. Regional-scale Grenvillian-age UHT metamorphism in the Mollendo–Camana Block (basement of the Peruvian Andes). Journal of Metamorphic Geology 21 (1), 99–120.

Martignole, J., Stevenson, R., Martelat, J.E., 2005. A Grenvillian anorthosite–mangerite–charnockite–granite suite in the basement of the Andes: the Ilo AMCG site (southern Peru). IDSAG, Barcelona, Extended, pp. 481–484.

McDonough, M.R., Ramos, V.A., Isachsen, C.E., Bowring, S.A., Vujovich, G.I., 1993. Edades preliminares de circones del basamento de la Sierra de Pie de Palo, Sierras Pampeanas occidentales de San Juán: sus implicancias para el supercontinente proterozoico de Rodinia: XII Congreso Geológico Argentino y II Congreso de Exploración de Hidrocarburos, Mendoza. Actas 3, 340–342.

Nelson, B., DePaolo, D.J., 1988. Comparison of isotopic and petrographic provenance indicators in sediments from Tertiary continental basins of New Mexico. Journal of Sedimentary Petrology 58 (2), 348–357.

Pankhurst, R.J., Rapela, C.W., 1998. The proto-Andean margin of Gondwana: an introduction. In: Pankhurst, R.J., Rapela, C.W. (Eds.), The Proto-Andean margin of Gondwana. Geological Society of London Special Publication, vol. 142, pp. 1–9.

Piper, J.D.A., 1976. Palaeomagnetic evidence for a Proterozoic supercontinent. Philosophical Transactions of the Royal Society of London A280, 469–490.

Porcher, C.C., Fernandes, L.A.D., Vujovich, G.I., Chernicoff, C.J., 2004. Thermobarometry, Sm/Nd ages and geophysical evidence for the location of the suture zone between Cuyania and Pampia terranes. Gondwana Research Special Issue 7 (4), 1057–1076.

Ramos, V.A., 1988. Late Proterozoic–Early Paleozoic of South America — a collisional history. Episodes 11, 168–174.

Ramos, V.A., 2004. Cuyania, an exotic block to Gondwana: review of a historical success and the present problems. In: Vujovich, G.I., Fernandes, L.A.D., Ramos, V., V.A. (Eds.), Cuyania: an exotic block to Gondwana. Gondwana Research Special Issue, vol. 7 (4), pp. 1009–1026.

Rapela, C.W., Pankhurst, R.J., Casquet, C., Baldo, E., Saavedra, J., Galindo, C., 1998a. Early evolution of the Proto-Andean margin of South America. Geology 26, 707–710.

Rapela, C.W., Pankhurst, R.J., Casquet, C., Baldo, E., Saavedra, J., Galindo, C., Fanning, C.M., 1998b. The Pampean orogeny of the southern Proto-Andes: a Cambrian continental collision. Evidence from the Sierras Pampenas de Cordoba (Argentina). Journal of the Geological Society of London Special Publication 142, 181–217.

Rapela, C.W., Pankhurst, R.J., Casquet, C., Fanning, C.M., Galindo, C., Baldo, E., 2005. Datación U–Pb SHRIMP de circones detríticos en para-anfibolitas neoproterozoicas de la secuencia Difunta Correa (Sierras Pampeanas Occidentales, Argentina). Geogaceta 38, 227–230.

Roback, R.C., James, E.W., Whitefield, C., Connely, J., 1995. Tectonic assembly of "Grenville" terrane in the Llano Uplift, central Texas, evidence from Pb and Sm–Nd isotopes. Abstracts with Programs. Geological Society of America 27 (6), 398.

Shackleton, R.M., Ries, A.C., Coward, M.P., Cobbold, P.R., 1979. Structure, metamorphism and geochronology of the Arequipa massif of coastal Peru. Journal of the Geological Society of London 136, 195–214.

Stacey, J., Kramers, J., 1975. Approximation of terrestrial lead isotope evolution by a two-stage model. Earth and Planetary Science Letters 26, 207–221.

Thomas, W.A., Astini, R.A., 1996. The Argentine Precordillera, a traveler from the Ouachita Embayment of North American Laurentia. Science 273, 752–757.

Tosdal, R.M., 1996. The Amazon–Laurentian connection as viewed from the Middle Proterozoic rocks in the Central Andes, western Peru and Northern Chile. Tectonics 15, 827–842.

Tosdal, R.M., Bettencourt, J.S., 1994. U–Pb zircon ages and Pb isotopic compositions of Middle Proterozoic Rondonian Massif, southwestern margin of the Amazon craton, Brazil. Actas VII Geological Congress of Chile, Actas, II, pp. 1538–1541.

Varela, R., Valencio, S., Ramos, A., Sato, K., González, P., Panarello, H., Roverano, D., 2001. Isotopic strontium, carbon and oxygen study on Neoproterozoic marbles from Sierra de Umango, and their foreland, Argentina. III South American Symposium on Isotope Geology 450–453.

Varela, R., Basei, M., Sato, A., Siga Jr., O., 2003. Proterozoico medio y Paleozoico inferior de la sierra de Umango, antepais andino (29 °S), Argentina: edades U–Pb y caracterizaciones isotópicas. Revista de la Sociedad Geologica de Chile 30, 265–284.

Vujovich, G.I., Kay, S.M., 1998. A Laurentian? Grenville-age oceanic arc/back-arc terrane in the Sierra de Pie de Palo, Western Sierras Pampeanas, Argentina. In: Pankhurst, R.J., Rapela, C.W. (Eds.), The Proto-Andean margin of Gondwana. Geological Society of London Special Publication, vol. 142, pp. 159–179.

Vujovich, G.I., Van Staal, C.R., Davis, W., 2004. Age constraints and the tectonic evolution and provenance of the Pie de Palo Complex, Cuyania composite terrane, and the Famatinian orogeny in the Sierra de Pie de Palo, San Juán, Argentina. Gondwana Research Special Issue 7 (4), 1041–1056.

Wareham, C.D., Pankhurst, R.J., Thomas, R.J., Storey, B.C., Grantham, G.H., Jacobs, J., Eglington, B.M., 1998. Pb, Nd and Sr isotope mapping of Grenville-age crustal provinces in Rodinia. Journal of Geology 106, 647–659.

Wasteneys, H.A., Clark, A.H., Farrar, E., Lagridge, R.J., 1995. Grenvillian granulite-facies metamorphism in the Arequipa Massif, Peru: a Laurentia–Gondwana link. Earth and Planetary Science Letters 132, 63–73.

Wingate, M.T.D., Campbell, I.H., Compston, W., Gibson, G.M., 1998. Ion microprobe U–Pb ages for Neoproterozoic-basaltic magmatism in south-central Australia and implications for the breakup of Rodinia. Precambrian Research 87, 135–159.